INTERNATIONAL JOURNAL OF HYDROGEN ENERGY 45 (2020) 33648–33656

Available online at www.sciencedirect.com

ScienceDirect

journal homepage: www.elsevier.com/locate/he

Deposition of an ultrathin palladium (Pd) coating on SAPO-34 membranes for enhanced H_2/N_2 separation

Ji Jiang [a], *Syed Islam* [a], *Qiaobei Dong* [a], *Fanglei Zhou* [a], *Shiguang Li* [b], *Miao Yu* [a,*]

[a] *Department of Chemical & Biological Engineering, Rensselaer Polytechnic Institute, Troy, NY, 12180, USA*
[b] *Gas Technology Institute, 1700 S Mount Prospect Road, Des Plaines, IL, 60018, USA*

HIGHLIGHTS

- An ultrathin Pd coating was deposited on SAPO−34 membranes.
- The composite membrane showed enhanced H_2/N_2 selectivity.
- The composite membrane showed comparable H_2 permeance to fresh SAPO−34 membrane.
- The Pd/SAPO−34 composite membrane showed high stability.

ARTICLE INFO

Article history:
Received 21 July 2020
Received in revised form
10 September 2020
Accepted 11 September 2020
Available online 30 September 2020

Keywords:
Zeolite membrane
H_2/N_2 separation
Pd coating
Pd/SAPO-34 composite membrane

ABSTRACT

Hydrogen energy has attracted great attention due to its properties of high energy transferring efficiency and zero pollution emission. Zeolite membranes are promising candidates for H_2 separation because of their uniform, molecular-sized pores and high thermal and mechanical stabilities. However, thicker membranes or modification treatments are often necessary to eliminate the defects formed during synthesis and post calcination, leading to low gas permeance. Herein, we reported the deposition of an ultrathin palladium (Pd) coating on SAPO-34 membranes to improve H_2 separation performance. H_2/N_2 selectivity was greatly increased by deposition of an ultrathin Pd coating on SAPO-34 membranes, while maintaining similar H_2 permeance. This might be attributed to the dissociative adsorption and associative desorption of H_2 on Pd, as well as fast diffusion of H_2 through ultrathin Pd coating. We also noticed that excessive Pd deposition would lead to the formation of cracks on SAPO-34 membranes, leading to deteriorated membrane performance.

Introduction

Hydrogen production and purification has attracted great attention due to the properties of high energy transferring efficiency and zero pollution emission of hydrogen energy [1–4]. Especially, the demand of high-purity H_2 for proton-exchange membrane (PEM) fuel cell requires new techniques for H_2 production with higher separation efficiency and lower

* *Corresponding author.*
E-mail address: yum5@rpi.edu (M. Yu).
https://doi.org/10.1016/j.ijhydene.2020.09.087

cost [5,6]. In recent few decades, membrane-based separation technique has attracted great attention due to its easy operation, low energy consumption, and cost effectiveness even at low gas volumes [7–11]. Among several types of membranes, palladium (Pd)-based membranes [12], silica membranes [13], MOF membranes [14], and zeolite membranes [9] were widely studied for H_2 separation and purification. However, the high cost of Pd membranes [12], strict preparation procedure of silica membranes [13], and poor thermal stability of MOF membranes [15] at high temperature limited the wide applications of these membranes. In contrast, zeolite membranes showed many advantages for H_2 separation and purification, such as well-defined pores, excellent thermal resistance and mechanical and chemical stability [16,17].

Till now, several kinds of zeolite membranes have been studied for H_2 separation from other gases [18–25]. Since the molecular sizes of H_2 and N_2 are 0.289 and 0.364 nm, respectively, zeolite membranes with small pore size, especially those with pore size <0.37 nm [20,23], are expected to be more efficient for H_2/N_2 separation. However, most of those membranes showed either low H_2 selectivity or low H_2 permeance, which could be attributed to the strongly negatively charged surface of Al-rich zeolites or the mismatch of the thermal expansion coefficients between the zeolite layer and the ceramic or metal support upon drying the as-synthesized membranes [26]. For high-silica zeolite membranes, such as DDR, the low performance might be attributed to the difficulty in remaining integrated structure of the membrane during structure directing agent removal [23,27]. In recent years, researchers noticed that SAPO-34 membranes with CHA topology usually showed high H_2 permeance with decent H_2/N_2 selectivity [7,24,25]. The H_2 permeance of SAPO-34 membrane can be as high as 9×10^{-6} mol m^{-2} s^{-1} Pa^{-1} while the H_2/N_2 selectivity could be as high as 20 [25], making it very attractive for H_2 production and separation from other gases.

Although zeolite membranes showed great potential for H_2 separation from other gases, almost inevitable grain boundary defects or cracks, formed during hydrothermal synthesis and/or thermal treatment required for removing structure directing agents (SDAs), make it difficult to achieve high H_2 selectivity and purity [28–30]. Therefore, posttreatments were usually necessary to improve the selectivity [30–39], such as modification of zeolite pores and/or non-zeolitic pores by catalytic cracking deposition of silane [37,38] and deposition of amorphous aluminum alkoxide [39]. Nevertheless, these treatments usually led to ultra-low gas permeance [37–39], which makes them less attractive for H_2 separation and purification.

Pd-based membranes usually showed high H_2 permeance and high H_2 selectivity to other gases [40–42], because of the dissociative adsorption and associative desorption of H_2, as well as diffusion of H_2 through Pd particles and the membrane layer [43,44]. Previous work also indicated that it was an effective way of improving H_2 selectivity by preparing Pd/zeolite composite membranes [36,45–48]. Nevertheless, besides the complex preparation procedure [36,46], H_2 permeance was also significantly reduced as compared with fresh zeolite membranes [36,45–47]. The low permeance might be attributed to the Pd particle distribution through the whole zeolite membrane layer by the improper Pd deposition technique [45,46], which greatly increased the mass transfer resistance.

Herein, we reported a novel strategy for modification of SAPO-34 membranes by deposition of an ultrathin Pd coating only on the membrane surface. Great improvement on H_2/N_2 selectivity with negligible decrease of H_2 permeance was achieved by controlling the deposition times and aggregation degree. We expect that this would be a new way of improving the selectivity of H_2 selective zeolite membranes.

Experimental

Chemicals and materials

Ludox AS-40 colloidal silica (SiO_2, 40 wt %), phosphoric acid (H_3PO_4, 85 wt %), aluminum isopropoxide (Al (i-$C_3H_7O)_3$, 99.99%), sodium hydroxide (NaOH, 98%), tetraethylammonium hydroxide (TEAOH, 35 wt% aqueous solution), dipropylamine (DPA, 99%), palladium (II) acetate (98%), and acetone (99.9%) were purchased from Sigma-Aldrich. All chemicals were used as received.

Membranes preparation

SAPO-34 membranes were hydrothermally synthesized onto the external surface of 4-channel α-Al_2O_3 hollow fiber support (O.D.: 3.6 mm; cylindrical channel I.D.: 0.9 mm; length: 80 mm; porosity: ~40%; average pore size: ~0.5 μm) that was used in our previous work [49] by secondary growth method. Prior to seeding, the hollow fiber support was treated in 2 M NaOH solution overnight to remove impurities, then thoroughly washed with distilled water to remove residual NaOH, and finally dried at 80 °C overnight. Both ends of the support were sealed by Teflon tape and then dipped into SAPO-34 seed suspension (2 wt%) containing 2 wt% colloidal silica for 10 s. Detailed information about seed preparation could be found in our previous work [50]. Six seeded hollow fibers were bundled onto a Teflon holder with uniform distribution and dried at 80 °C for 2 h. Finally, hollow fibers loaded on Teflon holder were placed vertically in Teflon-lined stainless-steel autoclave (Parr digestion bomb model 4744) for membrane synthesis at 200 °C for 24 h.

The gel was stirred at room temperature for 5 days before it was used for membrane growth. The corresponding molar ratio of the membrane synthesis gel was 1.0 Al_2O_3: 1.0 P_2O_5: 0.5 SiO_2: 1.0 TEAOH: 1.6 DPA: 150H_2O. Detailed information about the precursor and membrane preparation could be referred to our previous work [51]. After synthesis, the autoclave was quenched with tap water, and the synthesized membranes were washed with distilled water and dried at 80 °C overnight. The membranes were then calcined at 500 °C for 6 h with both heating and cooling rates of 1.0 °C/min, respectively. All membranes were stored at 220 °C before gas permeation measurements.

Pd deposition on SAPO-34 membranes

5.0 g/L palladium (II) acetate in acetone solution was used for the deposition of thin Pd coating on SAPO-34 membranes. The

deposition of thin Pd coating layer on SAPO-34 membranes was carried out by dip coating method using a dip coater. The coating speed was controlled at 5 mm/min. After each coating, Pd coated SAPO-34 membranes were dried at 120 °C for 2 h. The coating process was repeated for 1 to 10 times. Finally, the Pd coated SAPO-34 membranes were calcined at 500 °C for 2 h with both heating and cooling rates of 1.0 °C/min, respectively. Schematics for the deposition of thin Pd layer on SAPO-34 membrane was shown in Fig. 1.

Gas permeation test

For gas permeation test, one end of the membrane was sealed with epoxy and the other end was glued together with a $\frac{1}{4}$-inch stainless steel tubing (Swagelok) using epoxy. Then, it was mounted into a stainless-steel module. Schematics and a photograph of the membrane module were shown in Fig. S1. Before gas permeation test, the membrane module was heated at 250 °C for 3 h to remove adsorbed water in SAPO-34 and Pd/SAPO-34 membranes. The Pd/SAPO-34 membrane was reduced at 250 °C for over 2 h using equimolar H_2/N_2 mixture before separation test. The feed pressure was modulated by a back-pressure regulator, and the permeate side was operated under atmospheric pressure. The gas permeation rate was measured by a bubble flow meter. For separation of binary gas mixtures, the total feed flow was 250 standard cubic centimeters per min (sccm), and no sweep gas was used on the permeate side. The compositions of the permeate and retentate streams were measured using a gas chromatograph every 10 min and each point was tested for over 2 h.

Permselectivity (ratio of permeances) was reported in this work. The permeance was calculated as the flux divided by the partial pressure difference for the component. Detailed information about the calculation of permeance and selectivity could refer to our previous work [50].

Characterizations

The morphology of SAPO-34 and Pd/SAPO-34 membranes was characterized by field emission scanning electron microscopy (FE-SEM, Carl Zeiss Supra 55) and transmission electron microscopy (TEM, JEOL JEM-2011). Zeolite structure was confirmed by X-ray diffraction (XRD, Bruker D8-Discover, Rigaku) with Cu K_α radiation in the 2θ range of 5–50°. Elemental composition of the membranes was analyzed by electron diffraction spectroscopy (EDS, Oxford INCA). The thickness of Pd coating and particle size of Pd were characterized by focused ion beam scanning electron microscopes (FIB-SEM, Zeiss Crossbeam FIB-SEM). X-ray photoelectron spectroscopy (XPS) measurements of Pd/SAPO-34 membranes were carried out on an XPS system using an Al Kα X-ray gun of a spectral resolution < 0.5 eV.

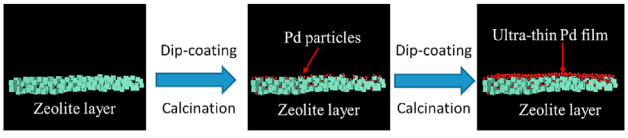

Fig. 1 – Schematics of the deposition of ultrathin Pd layer on SAPO-34 membrane.

Results and discussion

Membrane characterizations

Surface and cross-sectional SEM images of a SAPO-34 membrane were shown in Fig. 2. Well-crystalline SAPO-34 membrane layer with crystal size and thickness of 1–4 μm and 7.5 μm, respectively, could be observed. XRD result (Fig. 3a) confirmed pure phase of SAPO-34. The SAPO-34 membranes showed an average H_2 permeance of 3.85×10^{-7} mol m^{-2} s^{-1}·Pa^{-1} with H_2/N_2 selectivity of 7.6 for equimolar H_2/N_2 mixture gas separation, as shown in Table S1. For equimolar CO_2/CH_4 separation at room temperature and 0.1 MPa pressure drop across the membrane, an average CO_2/CH_4 selectivity of ca. 75 was obtained (data not shown here). These membranes showed comparable H_2/N_2 selectivity and CO_2/CH_4 selectivity as compared with most SAPO-34 membranes synthesized following similar procedure and reported in literature [7,52–55]. Note that high-quality SAPO-34 membranes with H_2/N_2 selectivity of >20 have been prepared by a novel gel-modulated growth method according to our very recent work [51]. These results suggest that the SAPO-34 membranes synthesized in this work might have more defects within the membrane layer. Therefore, appropriate post-treatments of SAPO-34 membranes seem to be necessary to improve H_2/N_2 selectivity.

In this work, we reported the deposition of an ultrathin Pd coating on SAPO-34 membranes to improve H_2/N_2 separation performance, as H_2 could pass through Pd layer by dissociative adsorption and associative desorption as well as diffusion, whereas other gases cannot [43,44]. To confirm our thought, the deposition of an ultrathin Pd coating on SAPO-34 membranes with different coating times by dip-coating was shown in Fig. S2. The coating color deepened with the increase of coating times from 1 to 10, suggesting more Pd was gradually deposited onto the surface of SAPO-34 membranes. After H_2 reduction, the color of the composite membranes changed from yellowish-brown to silver gray, suggesting the change in valence of Pd from Pd (II) to Pd (0) [45,56]. To confirm the formation of ultrathin Pd coating/Pd particles on SAPO-34 membranes, the composite membranes were characterized by TEM, SEM and FIB-SEM techniques, as shown in Fig. 4 and Fig. S3. Ultra-small Pd particles with particle size of 1–2 nm could be observed on SAPO-34 crystals after one-time coating (Fig. S3a). Nevertheless, aggregation of Pd particles was observed at the edge of SAPO-34 crystals (Fig. 4a), especially at the boundary of different crystals. Fig. 4b shows the thickness of Pd layer on SAPO-34 after one-time coating. The thickness varied from ca. 11–23.6 nm at different locations, suggesting non-uniformity of the Pd coating on the membrane surface, which was also confirmed by TEM images (Fig. S3). EDX result also suggested that Pd particles were mainly located at the boundaries of zeolite crystals (Fig. S4, the small dots in baby blue indicates Pd). Therefore, only one-time coating was not enough for full coverage of the surface of SAPO-34 membranes. When coating times increased to two, more Pd

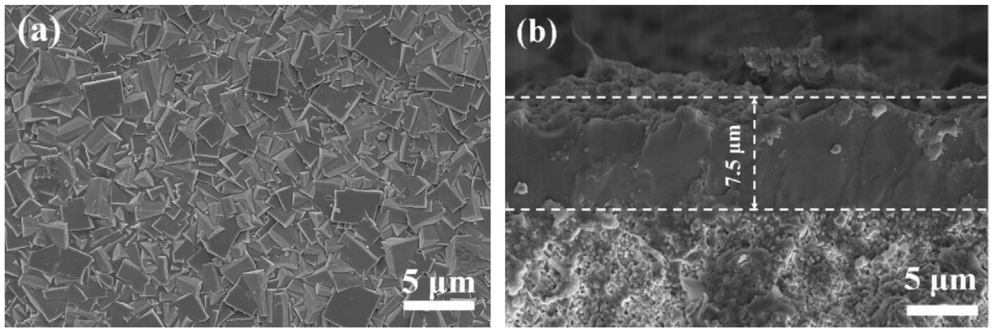

Fig. 2 – SEM images of surface (a) and cross-section (b) of SAPO-34 membrane.

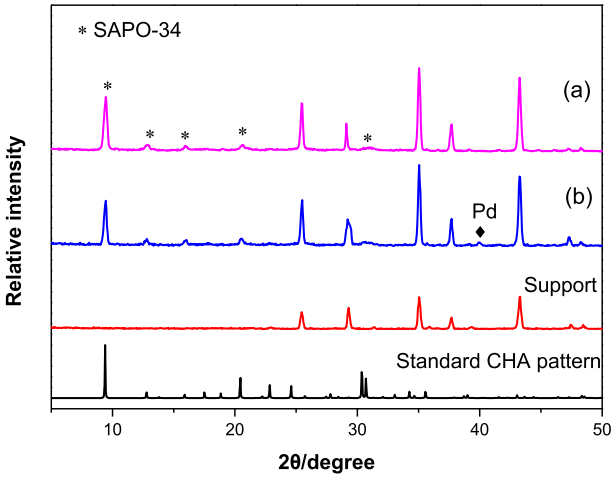

Fig. 3 – XRD patterns of fresh SAPO-34 membrane (a) and Pd particles deposited SAPO-34 membrane (b).

particles could be observed on the membrane surface (Fig. 4c). Besides, the Pd coating became more uniform and the thickness of this layer increased to ca. 21 nm (Fig. 4d). Further increase of Pd coating times did not lead to thicker Pd layer and larger Pd particle size on the membranes (Fig. 4f and h). However, cracks were observed on the membrane surface with more times of Pd coating (Fig. 4e and g), which might be related to the aggregation of small Pd particle at the edge and in the grain boundary of zeolite crystals and thus an unmatched mechanical stress between Pd particles and zeolite crystals. To understand the formation of cracks during coating, SAPO-34 membranes were treated with the solvent acetone only following the same procedure as Pd deposition on the membrane for 10 times or directly immersed in pure acetone for 2 days. Finally, those membranes were calcined using the same procedure as Pd/SAPO-34 membranes. We did not observe obvious changes of the membrane separation performance (both H_2 permeance and H_2/N_2 selectivity, data not shown here) and the surface microstructure (Fig. S5) after either treatment, suggesting that the formation of cracks was mainly attributed to the aggregation of Pd particles in grain boundary defects and at the edge of zeolite crystals.

XRD pattern of Pd/SAPO-34 membrane was shown in Fig. 3b. The relative peak intensity of SAPO-34 crystals was not affected by Pd coating, which could be related to the ultrathin Pd layer. A small peak at 2θ of ca. 40° could be observed for Pd/SAPO-34 membrane, indicating the formation of metallic Pd layer on SAPO-34 membrane surface [45,46]. Fig. 5 shows the XPS spectra of the Pd 3 d region of the Pd/SAPO-34 membrane before and after H_2/N_2 separation test. Before H_2/N_2 separation test, the major peak values for Pd $3d_{5/2}$ at 335.9 and 341.1 eV could be attributed to its oxidation state of Pd (II), which could be related to membrane calcination in air. After H_2/N_2 separation test at 250 °C for 1 h, peak values at 333.3 and 338.7 eV could be attributed to the formation of Pd (0) and a state between Pd (0) and Pd (II) [45]. These results indicated that Pd (II) was only partially reduced to Pd (0) after the H_2/N_2 separation test or the reduced Pd (0) was partially oxidized to Pd (II) after exposure to air.

Gas permeation test

Since H_2 could pass through dense Pd metal while other gases cannot, an ultrathin Pd layer might be helpful for improving H_2 selectivity by inhibiting the transport of other gases through the membrane. To demonstrate this, both single gas and mixture gas permeation through fresh SAPO-34 membrane and Pd/SAPO-34 membrane (2 times of coating) were measured at room temperature (22 °C) and 250 °C and pressure of 10 bar. At room temperature (Fig. 6a), all the gas permeances were severely affected by Pd deposition on SAPO-34 membranes. This could be explained by the increase of mass transfer resistance by the Pd coating. At higher temperature of 250 °C, H_2 permeance of Pd/SAPO-34 membrane greatly increased to >95% of the fresh SAPO-34 membrane. Nevertheless, permeation of other gases was still affected by Pd deposition. At higher temperature, H_2 could dissociate on Pd particles and pass through the thin Pd layer, leading to the increased H_2 permeance. The relatively high permeance of He could be attributed to small molecular size of He and the defects on Pd/SAPO-34 membrane as the ultrathin Pd coating is not dense. For other gases, it would be still difficult for them to pass through the Pd layer. Therefore, low permeance as compared with SAPO-34 membranes was found. Besides, the penetration of ultra-small Pd particles into the defects of SAPO-34 membranes also led to the decrease of gas permeation through non-zeolitic pores, leading to increased H_2 selectivity of the composite membranes.

Fig. 7 presents the effect of Pd coating times on the H_2/N_2 separation performance of the composite Pd/SAPO-34 membranes at 250 °C and pressure of 10 bar. H_2 permeance decreased with the increase of Pd coating times on the

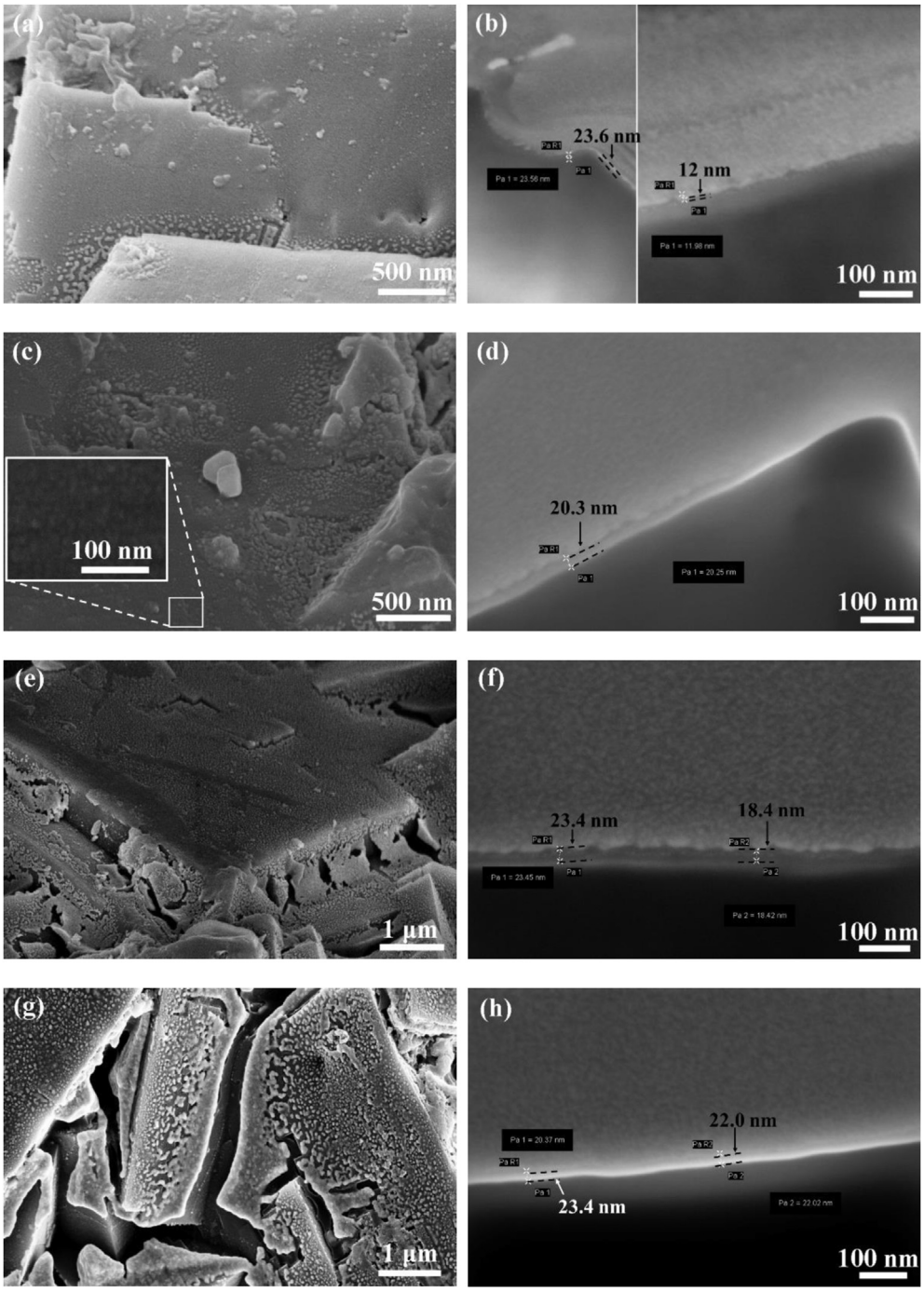

Fig. 4 – SEM and FIB-SEM images of Pd/SAPO-34 composite membranes after various Pd coating times: 1 (a, b), 2 (c, d), 4 (e, f) and 8 (g, h).

membrane, which could be related to the increase of mass transfer resistance on the membrane surface and blockage of non-selective pores upon Pd deposition. Nevertheless, H_2/N_2 selectivity increased after 2 times of coating and then decreased with further increase of coating time. With less or equal to two times of coating, a relatively uniform Pd layer gradually formed on SAPO-34 membranes, leading to the faster reduction of N_2 permeance than that of H_2 and thus increased H_2/N_2 selectivity. However, severe aggregation of ultra-small Pd particles occurred on the membrane surface with more coating times, leading to non-continuity of the Pd coating layer and thus decreased H_2/N_2 selectivity. What's worse was the aggregation of nano-sized Pd particles in defects led to the formation of cracks between zeolite crystals (Fig. 4e and g). Therefore, H_2/N_2 selectivity of the composite membranes decreased quickly with further deposition of Pd particles on the membrane surface.

Fig. 8 presents the results of H_2/N_2 mixture separation through SAPO-34 membrane and Pd/SAPO-34 membrane after two times of Pd coating as a function of permeation

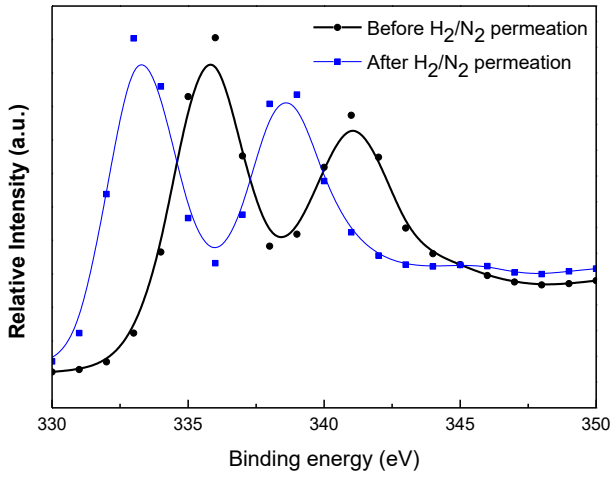

Fig. 5 – Fitted spectra for the Pd 3 d region of the Pd/SAPO 34 membrane before and after H_2/N_2 separation test.

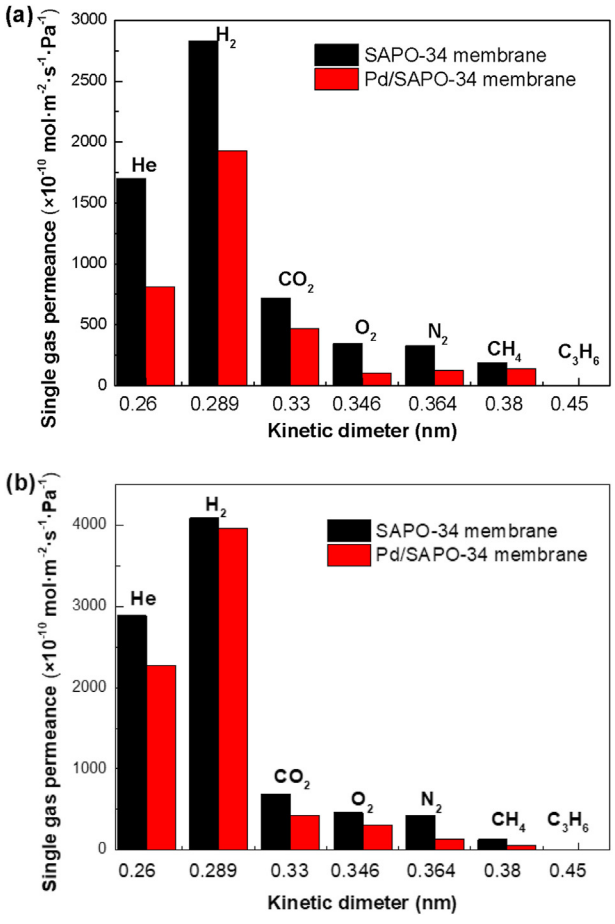

Fig. 6 – Single-gas permeation through SAPO/34 membrane and Pd/SAPO-34 composite membrane after 2 times of Pd coating at room temperature (a) and 250 °C (b).

temperature. H_2 permeance increased with temperature for both fresh SAPO-34 membrane and Pd/SAPO-34 membrane. Since H_2 adsorption on SAPO-34 was very weak, transport of H_2 through the membrane was dominated by diffusion. Therefore, H_2 permeance increased with temperature in both

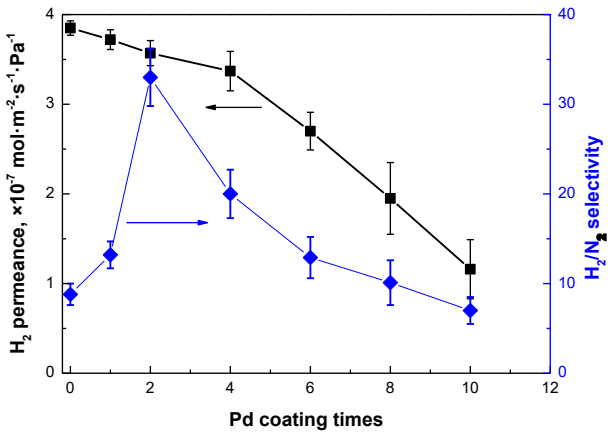

Fig. 7 – Effect of Pd coating times on the separation performance of Pd/SAPO-34 membranes for equimolar H_2/N_2 mixture at 250 °C and pressure of 10 bar.

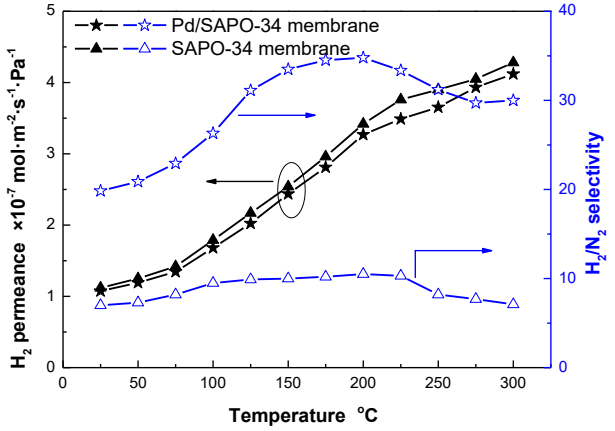

Fig. 8 – Equimolar H_2/N_2 separation through SAPO-34 membrane and Pd/SAPO-34 composite membrane with two times of Pd coating as a function of permeation temperature at feed pressure of 10 bar.

cases. H_2/N_2 selectivity of SAPO-34 membrane increased

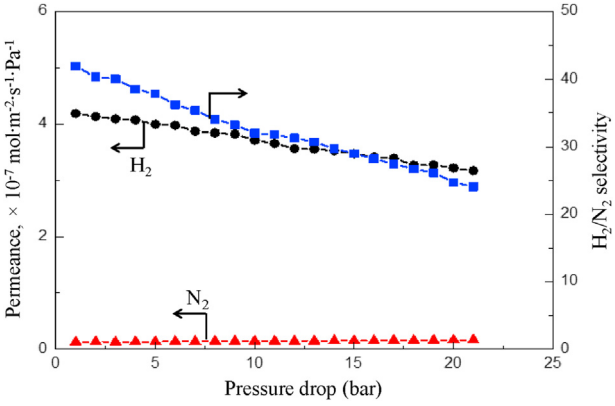

Fig. 9 – Equimolar H_2/N_2 mixture separation through Pd/SAPO-34 membrane as a function of pressure drop at 250 °C.

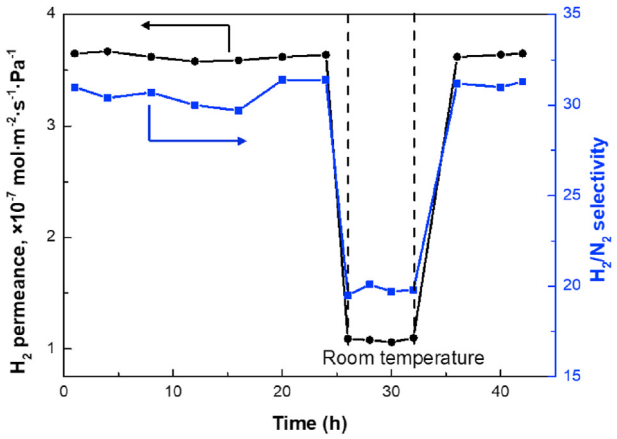

Fig. 10 – Long-term stability test of Pd/SAPO-34 membrane with 2 times of Pd coating for equimolar H_2/N_2 separation at 250 °C and 10 bar feed pressure.

slightly with temperature, and it was always below 11, which could be related to the existence of defects within the membrane layer. For Pd/SAPO-34 membrane, it showed comparable permeance to fresh SAPO-34 membrane, but H_2/N_2 selectivity greatly increased at temperature below 200 °C, indicating that most of large defects were blocked by nano-sized Pd particles and N_2 permeation was blocked by the ultra-thin Pd coating on the membrane surface. Finally, a high H_2/N_2 selectivity of ca. 35 was obtained at 175 °C.

Fig. 9 presents the results of equimolar H_2/N_2 mixture separation through Pd/SAPO-34 membrane as a function of pressure drop at 250 °C. N_2 permeance was almost not affected by the pressure drop, whereas H_2 permeance decreased near linearly with pressure, leading to a continuous decrease of H_2/N_2 selectivity with the increase of pressure drop. This suggests that the permeation behavior of the composite Pd/SAPO-34 membrane was not affected by the ultrathin Pd coating layer on SAPO-34 membrane. This could be attributed to the ultrathin Pd coating layer (ca. 20 nm), which had negligible influence on H_2 permeation. Besides, the relatively low temperature might also affect the H_2 adsorption and desorption on Pd particles, leading to less significant H_2 permeance decrease with pressure drop than Pd metal membranes [57,58].

To further demonstrate the stability of the composite Pd/SAPO-34 membrane, long-term testing of equimolar H_2/N_2 separation was carried out at 250 °C and 10 bar feed pressure. As shown in Fig. 10, the membrane showed stable performance at 250 °C for over 30 h. After cooling down to room temperature for several h and tested again at 250 °C, no obvious difference in H_2 permeance and H_2/N_2 selectivity was observed, suggesting that the ultrathin Pd layer was stable on SAPO-34 membrane. We expect that the composite Pd/SAPO-34 membranes can be used at higher temperature for other purposes, such as hydroxylation and dehydrogenation of organics.

Conclusions

In this work, an ultrathin Pd layer was deposited onto the surface of SAPO-34 membranes by a simple dip-coating method. The composite Pd/SAPO-34 membranes showed enhanced H_2/N_2 selectivity while maintaining comparable H_2 permeance to the fresh SAPO-34 membranes at 250 °C, which could be related to the blockage of N_2 by the ultrathin Pd layer. Besides, the membranes showed improved performance with temperature and was stable at 250 °C for over 30 h. Excellent long-term membrane stability and membrane stability to temperature variation (250 °C → 20 °C → 250 °C) was also demonstrated. We expect this new strategy might be applied for improving other inorganic membranes for H_2 separation.

Declaration of competing interest

The authors declare that they have no known competing financial interests or personal relationships that could have appeared to influence the work reported in this paper.

Acknowledgements

We thank the Advanced Research Projects Agency-Energy (ARPA-E) of Department of Energy (DOE) for the financial support under contract of DE-AR0000931; Rensselaer Polytechnic Institute (RPI) startup funds. We also sincerely thank Prof. Xuehong Gu at Nanjing Tech University for providing the α-Al_2O_3 hollow fiber support.

Appendix A. Supplementary data

Supplementary data to this article can be found online at https://doi.org/10.1016/j.ijhydene.2020.09.087.

REFERENCES

[1] Abe J, Ajenifuja E, Popoola O. Hydrogen energy, economy and storage: review and recommendation. Int J Hydrogen Energy 2019;44:15072–86. https://doi.org/10.1016/j.ijhydene.2019.04.068.

[2] Dincer I, Acar C. Review and evaluation of hydrogen production methods for better sustainability. Int J Hydrogen Energy 2015;40:11094–111. https://doi.org/10.1016/j.ijhydene.2014.12.035.

[3] Guo XM, Trably E, Latrille E, Carrere H, Steyer J-P. Hydrogen production from agricultural waste by dark fermentation: a review. Int J Hydrogen Energy 2010;35:10660–73. https://doi.org/10.1016/j.ijhydene.2010.03.008.

[4] Sgobbi A, Nijs W, De Miglio R, Chiodi A, Gargiulo M, Thiel C. How far away is hydrogen? Its role in the medium and long-term decarbonisation of the European energy system. Int J Hydrogen Energy 2016;41:19–35. https://doi.org/10.1016/j.ijhydene.2015.09.004.

[5] Jo YS, Cha J, Lee CH, Jeong H, Yoon CW, Nam SW, et al. A viable membrane reactor option for sustainable hydrogen production from ammonia. J Power Sources 2018;400:518–26. https://doi.org/10.1016/j.jpowsour.2018.08.010.
[6] Pearlman JB, Bhargav A, Shields EB, Jackson GS, Hearn P. Modeling efficiency and water balance in PEM fuel cell systems with liquid fuel processing and hydrogen membranes. J Power Sources 2008;185:1056–65. https://doi.org/10.1016/j.jpowsour.2008.08.057.
[7] Zhou L, Yang J, Li G, Wang J, Zhang Y, Lu J, Yin D. Highly H_2 permeable SAPO-34 membranes by steam-assisted conversion seeding. Int J Hydrogen Energy 2014;39:14949–54. https://doi.org/10.1016/j.ijhydene.2014.06.159.
[8] Phair JW, Badwal SPS. Materials for separation membranes in hydrogen and oxygen production and future power generation. Sci Technol Adv Mater 2006;7:792. https://doi.org/10.1016/j.stam.2006.11.005.
[9] Verweij H, Lin YS, Dong J. Microporous silica and zeolite membranes for hydrogen purification. MRS Bull 2006;31:756–64. https://doi.org/10.1557/mrs2006.189.
[10] Nenoff TM, Spontak RJ, Aberg CM. Membranes for hydrogen purification: an important step toward a hydrogen-based economy. MRS Bull 2006;31:735–44. https://doi.org/10.1557/mrs2006.186.
[11] Cheng YS, Peña MA, Fierro JL, Hui DCW, Yeung KL. Performance of alumina, zeolite, palladium, Pd-Ag alloy membranes for hydrogen separation from Towngas mixture. J Membr Sci 2002;204:329–40.
[12] Al-Mufachi NA, Rees NV, Steinberger-Wilkens R. Hydrogen selective membranes: a review of palladium-based dense metal membranes. Renew Sustain Energy Rev 2015;47:540–51. https://doi.org/10.1016/j.rser.2015.03.026.
[13] De Vos RM, Verweij H. High-selectivity, high-flux silica membranes for gas separation. Science 1998;279:1710–1. https://doi.org/10.1126/science.279.5357.1710.
[14] Guo H, Zhu G, Hewitt IJ, Qiu S. "Twin copper source" growth of metal-organic framework membrane: $Cu_3(BTC)_2$ with high permeability and selectivity for recycling H_2. J Am Chem Soc 2009;131:1646–7. https://doi.org/10.1021/ja8074874.
[15] Lin YS. Metal organic framework membranes for separation applications. Curr Opin Chem Eng 2015;8:21–8. https://doi.org/10.1016/j.coche.2015.01.006.
[16] Ozin GA, Kuperman A, Stein A. Advanced zeolite, materials science. Angew Chem Int Ed 1989;28:359–76. https://doi.org/10.1002/anie.198903591.
[17] Tavolaro A, Drioli E. Zeolite membranes. Adv Mater 1999;11:975–96. https://doi.org/10.1002/(SICI)1521-4095.199908)11:12<975::AID-ADMA975>3.0.CO;2-0.
[18] Michalkiewicz B, Koren ZC. Zeolite membranes for hydrogen production from natural gas: state of the art. J Porous Mater 2015;22:635–46. https://doi.org/10.1007/s10934-015-9936-6.
[19] Dong J, Lin YS. In situ synthesis of P-type zeolite membranes on porous α-alumina supports. Ind Eng Chem Res 1998;37:2404–9. https://doi.org/10.1021/ie970851o.
[20] Fasolin S, Romano M, Boldrini S, Ferrario S, Fabrizio M, Armelao L, et al. Single-step process to produce alumina supported hydroxy-sodalite zeolite membranes. J Mater Sci 2019;54:2049–58. https://doi.org/10.1007/s10853-018-2952-6.
[21] Korelskiy D, Ye P, Fouladvand S, Karimi S, Sjöberg E, Hedlund J. Efficient ceramic zeolite membranes for CO_2/H_2 separation. J Mater Chem 2015;3:12500–6. https://doi.org/10.1039/c5ta02152a.
[22] Liu B, Zhang R, Du Y, Gao F, Zhou J, Zhou R. Highly selective high-silica SSZ-13 zeolite membranes for H_2 production from syngas. Int J Hydrogen Energy 2020;45:16210–8. https://doi.org/10.1016/j.ijhydene.2020.04.082.
[23] Goswami N, Bose A, Das N, Achary SN, Sahu AK, Karki V, et al. DDR zeolite membrane reactor for enhanced HI decomposition in IS thermochemical process. Int J Hydrogen Energy 2017;42:10867–79. https://doi.org/10.1016/j.ijhydene.2017.02.175.
[24] Das JK, Das N, Bandyopadhyay S. Highly selective SAPO 34 membrane on surface modified clay-alumina tubular support for H_2/CO_2 separation. Int J Hydrogen Energy 2012;37:10354–64. https://doi.org/10.1016/j.ijhydene.2012.03.102.
[25] Das JK, Das N, Bandyopadhyay S. Highly oriented improved SAPO 34 membrane on low cost support for hydrogen gas separation. J Mater Chem 2013;1:4966–73. https://doi.org/10.1039/C3TA01095C.
[26] Caro J, Albrecht D, Noack M. Why is it so extremely difficult to prepare shape-selective Al-rich zeolite membranes like LTA and FAU for gas separation? Separ Purif Technol 2009;66:143–7. https://doi.org/10.1016/j.seppur.2008.11.009.
[27] Yang S, Cao Z, Arvanitis A, Sun X, Xu Z, Dong J. DDR-type zeolite membrane synthesis, modification and gas permeation studies. J Membr Sci 2016;505:194–204. https://doi.org/10.1016/j.memsci.2016.01.043.
[28] Choi J, Jeong HK, Snyder MA, Stoeger JA, Masel RI, Tsapatsis M. Grain boundary defect elimination in a zeolite membrane by rapid thermal processing. Science 2009;325:590–3. https://doi.org/10.1126/science.1176095.
[29] Bonilla G, Tsapatsis M, Vlachos DG, Xomeritakis G. Fluorescence confocal optical microscopy imaging of the grain boundary structure of zeolite MFI membranes made by secondary (seeded) growth. J Membr Sci 2001;182:103–9. https://doi.org/10.1016/S0376-7388(00)00549-4.
[30] Xomeritakis G, Lai Z, Tsapatsis M. Separation of xylene isomer vapors with oriented MFI membranes made by seeded growth. Ind Eng Chem Res 2001;40:544–52. https://doi.org/10.1021/ie000613k.
[31] Zhang B, Wang C, Lang L, Cui R, Liu X. Selective defect-patching of zeolite membranes using chemical liquid deposition at organic/aqueous interfaces. Adv Funct Mater 2008;18:3434–43. https://doi.org/10.1002/adfm.200800054.
[32] Yan Y, Davis ME, Gavalas GR. Preparation of highly selective zeolite ZSM-5 membranes by a post-synthetic coking treatment. J Membr Sci 1997;123:95–103. https://doi.org/10.1016/S0376-7388(96)00206-2.
[33] Hirota Y, Watanabe K, Uchida Y, Egashira Y, Yoshida K, Sasaki Y, et al. Coke deposition in the SAPO-34 membranes for examining the effects of zeolitic and non-zeolitic pathways on the permeation and separation properties in gas and vapor permeations. J Membr Sci 2012;415:176–80. https://doi.org/10.1016/j.memsci.2012.04.050.
[34] Matsuda H, Yanagishita H, Negishi H, Kitamoto D, Ikegami T, Haraya K, et al. Improvement of ethanol selectivity of silicalite membrane in pervaporation by silicone rubber coating. J Membr Sci 2002;210:433–7. https://doi.org/10.1016/S0376-7388(02)00364-2.
[35] Nomura M, Yamaguchi T, Nakao S. Silicalite membranes modified by counterdiffusion CVD technique. Ind Eng Chem Res 1997;36:4217–23. https://doi.org/10.1021/ie970338a.
[36] Morón F, Pina MP, Urriolabeitia E, Menéndez M, Santamaría J. Preparation and characterization of Pd-zeolite composite membranes for hydrogen separation. Desalination 2002;147:425–31. https://doi.org/10.1016/S0011-9164(02)00638-0.
[37] Masuda T, Fukumoto N, Kitamura M, Mukai SR, Hashimoto K, Tanaka T, et al. Modification of pore size of MFI-type zeolite by catalytic cracking of silane and application to preparation of H_2-separating zeolite membrane. Microporous Mesoporous Mater 2001;48:239–45. https://doi.org/10.1016/S1387-1811(01)00358-4.
[38] Hong M, Falconer JL, Noble RD. Modification of zeolite membranes for H_2 separation by catalytic cracking of

methyldiethoxysilane. Ind Eng Chem Res 2005;44:4035–41. https://doi.org/10.1021/ie048739v.
[39] Yu M, Funke HH, Noble RD, Falconer JL. H_2 separation using defect-free, inorganic composite membranes. J Am Chem Soc 2011;133:1748–50. https://doi.org/10.1021/ja108681n.
[40] Sun GB, Hidajat K, Kawi S. Ultra thin Pd membrane on α-Al_2O_3 hollow fiber by electroless plating: high permeance and selectivity. J Membr Sci 2006;284:110–9. https://doi.org/10.1016/j.memsci.2006.07.015.
[41] Yun S, Oyama ST. Correlations in palladium membranes for hydrogen separation: a review. J Membr Sci 2011;375:28–45. https://doi.org/10.1016/j.memsci.2011.03.057.
[42] Gallucci F, Fernandez E, Corengia P, Annaland M. Recent advances on membranes and membrane reactors for hydrogen production. Chem Eng Sci 2013;92:40–66. https://doi.org/10.1016/j.ces.2013.01.008.
[43] Paglieri SN, Way JD. Innovations in palladium membrane research. Separ Purif Methods 2002;31:1–169. https://doi.org/10.1081/SPM-120006115.
[44] Johansson M, Skúlason E, Nielsen G, Murphy S, Nielsen RM, Chorkendorff I. Hydrogen adsorption on palladium and palladium hydride at 1 bar. Surf Sci 2010;604:718–29. https://doi.org/10.1016/j.susc.2010.01.023.
[45] Das JK, Das N. Mercaptoundecanoic acid capped palladium nanoparticles in a SAPO 34 membrane: a solution for enhancement of H_2/CO_2 separation efficiency. ACS Appl Mater Interfaces 2014;6:20717–28. https://doi.org/10.1021/am5045345.
[46] Liu X, Liu W, Li J, Zhang Y, Lang L, Ma L, et al. Reactive deposition of palladium nanoparticles onto zeolite membranes in supercritical CO_2. Ind Eng Chem Res 2010;49:8826–31. https://doi.org/10.1021/ie100655m.
[47] Kiadehi AD, Taghizadeh M, Rami MD. Preparation of Pd/SAPO-34/PSS composite membranes for hydrogen separation: effect of crystallization time on the zeolite growth on PSS support. J Ind Eng Chem 2020;81:206–18. https://doi.org/10.1016/j.jiec.2019.09.010.
[48] Wang X, Tan X, Meng B, Zhang X, Liang Q, Pan H, et al. TS-1 zeolite as an effective diffusion barrier for highly stable Pd membrane supported on macroporous α-Al_2O_3 tube. RSC Adv 2013;3:4821–34. https://doi.org/10.1039/C3RA23086D.
[49] Shi Z, Zhang Y, Cai C, Zhang C, Gu X. Preparation and characterization of α-Al_2O_3 hollow fiber membranes with four-channel configuration. Ceram Int 2015;41:1333–9. https://doi.org/10.1016/j.ceramint.2014.09.065.
[50] Huang Y, Wang L, Song Z, Li S, Yu M. Growth of high-quality, thickness-reduced zeolite membranes towards N_2/CH_4 separation using high-aspect-ratio seeds. Angew Chem Int Ed 2015;54:10843–7. https://doi.org/10.1002/ange.201503782.
[51] Jiang J, Dong Q, Zhou F, Xu W, Li S, Yu M. Gel-modulated growth of high-quality zeolite membranes. ACS Appl Mater Interfaces 2020;12:26095–100. https://doi.org/10.1021/acsami.0c07274.
[52] Poshusta JC, Tuan VA, Pape EA, Noble RD, Falconer JL. Separation of light gas mixtures using SAPO-34 membranes. AIChE J 2000;46:779–89. https://doi.org/10.1002/aic.690460412.
[53] Poshusta JC, Tuan VA, Falconer JL, Noble RD. Synthesis and permeation properties of SAPO-34 tubular membranes. Ind Eng Chem Res 1998;37:3924–9. https://doi.org/10.1021/ie980240b.
[54] Li S, Falconer JL, Noble RD. SAPO-34 membranes for CO_2/CH_4 separation. J Membr Sci 2004;241:121–35. https://doi.org/10.1016/j.memsci.2004.04.027.
[55] Li S, Falconer JL, Noble RD. SAPO-34 membranes for CO_2/CH_4 separations: effect of Si/Al ratio. Microporous Mesoporous Mater 2008;110:310–7. https://doi.org/10.1016/j.micromeso.2007.06.016.
[56] Witońska IA, Walock MJ, Binczarski M, Lesiak M, Stanishevsky AV, Karski S. Pd-Fe/SiO_2 and Pd-Fe/Al_2O_3 catalysts for selective hydrodechlorination of 2, 4-dichlorophenol into phenol. J Mol Catal Chem 2014;393:248–56. https://doi.org/10.1016/j.molcata.2014.06.022.
[57] Liu J, Bellini S, Nooijer N, Sun Y, Tanaka D, Tang C, et al. Hydrogen permeation and stability in ultra-thin Pdsingle bondRu supported membranes. Int J Hydrogen Energy 2020;45:7455–67. https://doi.org/10.1016/j.ijhydene.2019.03.212.
[58] Kim CH, Han JY, Kim S, Lee B, Lim H, Lee KY, et al. Hydrogen production by steam methane reforming in a membrane reactor equipped with a Pd composite membrane deposited on a porous stainless steel. Int J Hydrogen Energy 2018;43:7684–92. https://doi.org/10.1016/j.ijhydene.2017.11.176.